L_c for some j's, $j \in \{1, 2, \cdots, M\}$. Delete these columns from $\tilde{\mathcal{S}}_{L_e+1}(\mathcal{F})$ to form $\tilde{\mathcal{S}}'_{L_e+1}(\mathcal{F})$ of size $[N(L_e+1)] \times [M(L_e+1)+\sum_{j=1}^{M} L_{cj}]$. Similarly delete corresponding rows from $\mathbf{G}_{hd}$, which are zeros anyway, since they are given by $a_j(k)$ for $L_{cj}+L_e+1 \le k \le L_c+L_e$ (cf. (3-16)). It, therefore, follows from (3-14) and the discussion leading up to it that $\tilde{\mathcal{S}}'_{L_e+1}(\mathcal{F})$ is of full column rank iff $\mathcal{F}(z)$ is column-reduced (in addition to satisfying AS5)), leading to the conclusion that

$$\{\mathbf{J}_{cd} = 0 \Rightarrow \mathbf{G}_{hd} = 0\} \quad \Leftrightarrow \quad \tilde{\mathcal{S}}'_{L_e+1}(\mathcal{F}) \text{ is full column rank} \Leftrightarrow \mathcal{F}(z) \text{ is column reduced and irreducible.} \tag{3-21}$$

In summary, it has been shown that for FIR systems, under AS5), a finite length equalizer of the type (3-15) exists to yield (1-5) with $d = 1$ and $k_0 = 0$. If, in addition, $\mathcal{F}(z)$ is column reduced and AS1) and AS3) are satisfied, all the stationary points of J w.r.t. the equalizer coefficients are described by the stationary points of G w.r.t. the composite impulse response $\overline{h}_j(k)$; the latter possess no undesirable local minima. However, if $\mathcal{F}(z)$ is not column reduced, then under AS1), AS3), and AS5), all the stationary points of J w.r.t. the equalizer coefficients are described by the stationary points of G w.r.t. $\overline{h}_j(k)$ whenever the equalizer is doubly infinite.

IV. Iterative Source Extraction and Identifiability

The preceding discussion suggests an iterative solution (as in [3]) where we iterate on inputs one by one; this solution is summarized in Table I. Note that the solution is guaranteed to work only in the absence of noise, although simulation results given in [14] are quite good, even in considerable amount of noise. It follows from the preceding developments that, given $\mathcal{F}(z)$, the proposed iterative approach yields a $\mathcal{G}(z)$, where the two are related via

$$\mathcal{G}(z) = \mathcal{F}(z)\mathbf{DAP} \tag{4-1}$$

where $\mathbf{D}$ is an $M \times M$ "time-shift" diagonal matrix (recall k_0 in (2-5)), $\mathbf{A}$ is an $M \times M$ diagonal scaling matrix (recall d in (2-5)), and $\mathbf{P}$ is an $M \times M$ permutation matrix (recall j_0 in (2-5), where we don't "know" which input it refers to). Thus, we have the following basic identifiability results.

Theorem 1: Given the model (1-1) such that $\mathbf{n}(k) \equiv 0$ and conditions AS1)–AS4) hold true. Suppose that doubly infinite equalizers are used in the iterative procedure of Table I, and the record length tends to infinity. Then, this procedure yields a transfer function $\mathcal{G}(z)$ satisfying (4-1).

Theorem 2: Given the FIR model (1-1) such that $\mathbf{n}(k) \equiv 0$ and conditions AS1) and AS3) hold true. Suppose that the iterative source separation procedure of Table I is used, and the record length tends to infinity. Then, this procedure yields a transfer function $\mathcal{G}(z)$ satisfying (4-1) if one of the following holds:

1) AS5) holds true and doubly-infinite equalizers are used.
2) AS5) holds true, $\mathcal{F}(z)$ is column reduced, and FIR equalizers with $L_e \ge (2M-1)L_c - 1$ (cf., (3-15)) are used. □

References

[1] S. Mayrargue, "A blind spatio-temporal equalizer for a radio-mobile channel using the constant modulus algorithm (CMA)," in *Proc. IEEE 1994 ICASSP*, Adelaide, Australia, Apr. 19–22, 1994, pp. II-317–320.

[2] D. N. Godard, "Self-recovering equalization and carrier tracking in two-dimensional data communication systems," *IEEE Trans. Commun.*, vol. COM-28, pp. 1867–1875, Nov. 1980.

[3] J. R. Treichler and M. G. Larimore, "New processing techniques based on the constant modulus adaptive algorithm," *IEEE Trans. Acoust., Speech, Signal Processing*, vol. ASSP-33, pp. 420–431, Apr. 1985.

[4] G. J. Foschini, "Equalizing without altering or detecting data," *BSTJ*, vol. 64, pp. 1885–1911, Oct. 1985.

[5] I. Fijalkow, F. Lopez de Victoria, and C. R. Johnson, "Adaptive fractionally spaced blind equalization," in *Proc. IEEE DSP Workshop*, Yosemite, 1994, pp. 257–260.

[6] D. T. M. Slock, "Blind joint equalization of multiple synchronous mobile users using oversampling," in *Proc. 28th Asilomar Conf.*, Pacific Grove, CA, Nov. 1994, pp. 1154–1158.

[7] I. Fijalkow, A. Touzni, and C. R. Johnson, "Spatio-temporal equalizability under channel noise and loss of disparity," *Proc. GRETSI*, 1995.

[8] J. K. Tugnait, "Identification of multichannel linear non-Gaussian processes using higher-order statistics," in *Proc. 29th Asilomar Conf.*, Pacific Grove, CA, Oct./Nov. 1995, pp. 792–797.

[9] T. Kailath, *Linear Systems*. Englewood Cliffs, NJ: Prentice-Hall, 1980.

[10] E. D. Sontag, "On generalized inverses of polynomial and other matrices," *IEEE Trans. Automat. Contr.*, vol. AC-25, pp. 514–517, June 1980.

[11] S. Kung, T. Kailath, and M. Morf, "A generalized resultant matrix for polynomial matrices," in *Proc. 1976 IEEE Conf. Decision Contr.*, FL, Dec. 1976, pp. 892–895.

[12] B. D. O. Anderson and E. I. Jury, "Generalized Bezoutian and Sylvester matrices in multivariable linear control," *IEEE Trans. Automat. Contr.*, vol. AC-21, pp. 551–556, 1976.

[13] J. K. Tugnait, "Spatio-temporal signal processing for blind separation of multichannel signals," in *Digital Signal Processing Tech.*, J. Picone, Ed., *Proc. SPIE 2750*, 1996, pp. 88–103; in *Proc. SPIE Conf.*, Orlando, FL, Apr. 10–11, 1996.

[14] , "Blind equalization and channel estimation for multiple-input multiple-output communications systems," in *Proc. IEEE 1996 ICASSP*, Atlanta, GA, May 7–10, 1996, pp. 2443–2446.

Robust Beamforming for Interference Rejection in Mobile Communications

Jaume Riba, Jason Goldberg, and Gregori Vàzquez

***Abstract*—The problem of robust beamformer design for mobile communications applications in the presence of moving co-channel sources is addressed. A generalization of the optimum beamformer based on a statistical model accounting for source movement is proposed. The new method is easily implemented and is shown to offer dramatic improvements over conventional optimum beamforming for moving sources under a variety of operating conditions.**

I. Introduction

The increasing demand for mobile communications services over the past several years has motivated the need for more efficient use of the RF spectrum. Traditional approaches to sharing spectral resources include channel multiplexing techniques that exploit diversity in time, frequency, and/or code. Nevertheless, expected user demand is such that the use of *spatial* diversity to further improve spectral efficiency has recently received considerable attention [1]–[3] (and references

Manuscript received December 18, 1995; revised August 21, 1996. This work was supported in part by EEC Contract HCM/CHRXCT-930405.

The authors are with the Department of Signal Theory and Communications, Polytechnic University of Catalonia, E. T. S. E. Telecomunicació, Campus Nord UPC, 08034 Barcelona, Spain (e-mail: jriba@gps.tsc.upc.es; jason@gps.tsc.upc.es; gregori@gps.tsc.upc.es).

Publisher Item Identifier S 1053-587X(97)00527-8.

therein). Specifically, the use of antenna arrays in combination with signal processing algorithms at the basestation offer the possibility of exploiting the spatial dimension to separate multiple, cochannel users. This recent approach has been shown to provide increased channel capacity and wider area coverage. Array beamforming methods in such systems make use of the spatial dimension to combat interference, noise, and multipath fading of the desired signal.

In most cases, the beamformer is designed using data taken over some short time interval. The weights are then held constant over some generally longer interval before being updated in response to changes in the scenario. This may be due to the lack of a continually available beamformer reference and/or limited computational resources. Such is the case, for example, in the uplink (mobile to basestation) of temporal reference beamforming (TRB) systems [1]. The training sequence used in the design of the beamformer is only available over a small fraction of the entire data frame length. The resulting beamformer weights are frozen and used for the remainder of the frame despite changes in the scenario. Moreover, in both TRB and spatially referenced beamforming (SRB) systems, the use of frozen weights may be desired to avoid the additional complexity of continuous updating. Another example is found in time division duplex (TDD) systems when the uplink beamformer is used during the subsequent downlink (basestation to mobile) in an effort to improve reception at the mobile [2].

The minimum rate at which the beamforming weights are updated depends on the speed with which the scenario changes. The performance of some beamformers can be seriously degraded when this updating rate is not sufficiently high. Consider, for example, the use of the optimum, maximum output signal-to-noise-and-interference-ratio (SINR) beamformer when the additive sensor noise power is low compared with the desired signal-of-interest (SOI) power that., in turn, is lower than the power of the interfering signals-not-of-interest (SNOI's). The optimum beamformer will often place sharp, deep nulls at the SNOI directions of arrival (DOA's) in order to maximize output SINR. However, output SINR can be severely degraded if source movement is significant relative to the beamformer updating rate.

This paper considers the problem of robust beamformer design in the presence of sources that move over the interval during which its weights are held constant. A new method is proposed that is based on a generalization of the optimum beamformer employing a statistical model accounting for source movement. The resulting array response pattern possesses a broad mainlobe and broad nulls over the SOI and SNOI DOA's, respectively, and is therefore less sensitive to source motion. Like [4], such response patterns are obtained *without* estimation of SNOI DOA's. However, rather than explicitly imposing derivative constraints at the SNOI DOA nulls as in [4], the new design procedure adaptively allocates beamformer degrees of freedom.

II. Problem Formulation

Consider a single, narrowband, desired signal-of-interest (SOI) in the far-field of an array of M passive sensors in the presence of $N-1$ cochannel SNOI's and additive, white noise. The M-dimensional snapshot vector at snapshot time index k is modeled as a sum of desired, interfering, and noise components

$$\begin{aligned} &\mathbf{y}(k) = \mathbf{d}(k) + \mathbf{i}(k) + \mathbf{n}(k), \\ &\mathbf{d}(k) = \mathbf{a}(\theta_0(k))\ s_0(k), \quad \mathbf{i}(k) = \sum_{m=1}^{N-1} \mathbf{a}(\theta_m(k))\ s_m(k). \end{aligned} \tag{1}$$

$\theta_0(k)$ and $\theta_m(k),\ m \in \{1, \ldots, N-1\}$ denote the DOA's (with respect to the array's broadside) at time k of the single SOI and the $N-1$ SNOI's, respectively, whereas $\mathbf{a}(\cdot)$ denotes the $M \times 1$ steering vector as a function of DOA. $s_0(k)$ and $s_m(k),\ m \in \{1, \ldots, N-1\}$ represent the SOI and the $N-1$ SNOI's at time k. Last, $\mathbf{n}(k)$ denotes the $M \times 1$ additive, white noise vector at time k.

Assuming that all the sources are mutually uncorrelated, the correlation matrix of the array snapshot is given by

$$\mathbf{R}_y = E[\mathbf{y}\mathbf{y}^H] = \mathbf{R}_d + \mathbf{R}_{i+n}, \tag{2}$$

$$\mathbf{R}_d = \gamma_0\, \mathbf{a}(\theta_0)\mathbf{a}^H(\theta_0) \tag{3}$$

$$\mathbf{R}_{i+n} = \sum_{m=1}^{N-1} \gamma_m \mathbf{a}(\theta_m)\mathbf{a}^H(\theta_m) + \sigma^2\mathbf{I}$$

where $(\cdot)^H$ denotes conjugate transpose, and explicit dependence on the time index k has been and will be suppressed where possible. γ_0 and $\gamma_m,\ m \in \{1, \ldots, N-1\}$ denote the powers of the SOI and the $N-1$ SNOI's, respectively. σ^2 denotes the sensor noise power.

Next, consider $z = \mathbf{w}^H\mathbf{y}$ to be the output of a beamformer $\mathbf{w}$. The SINR at z is defined as

$$\text{SINR}[\mathbf{w}] = \frac{\mathbf{w}^H\mathbf{R}_d\mathbf{w}}{\mathbf{w}^H\mathbf{R}_{i+n}\mathbf{w}} = \frac{\gamma_0\left|\mathbf{w}^H\mathbf{a}(\theta_0)\right|^2}{\mathbf{w}^H\mathbf{R}_{i+n}\mathbf{w}}. \tag{4}$$

The optimum beamformer that maximizes SINR (and is proportional to the well-known minimum variance distortionless response beamformer) can be interpreted (to within a scale factor) as the solution to the following constrained minimization problem:

$$\mathbf{w}_o = \arg\min_{\mathbf{w}} \mathbf{w}^H\mathbf{R}_{i+n}\mathbf{w} \quad \text{subject to} \quad \mathbf{w}^H\mathbf{R}_d\mathbf{w} = \gamma_0. \tag{5}$$

It is not difficult to show from (2) that the above problem is equivalent to

$$\mathbf{w}_o = \arg\min_{\mathbf{w}} \mathbf{w}^H\mathbf{R}_y\mathbf{w} \quad \text{subject to} \quad \mathbf{w}^H\mathbf{R}_d\mathbf{w} = \gamma_0. \tag{6}$$

In practice, this formulation is preferred since $\mathbf{R}_y$, unlike $\mathbf{R}_{i+n}$, can be easily and consistently (in the statistical sense) estimated directly from the snapshot data. Generally, optimization problems of the form in (5) or (6) are solved via generalized eigenanalysis as in [3]. However, since $\text{rank}(\mathbf{R}_d) = 1$, the quadratic constraint can be replaced by the linear constraint $\mathbf{w}^H\mathbf{a}(\theta_0) = 1$. The optimum beamformer can then be expressed simply as

$$\mathbf{w}_o = \frac{\mathbf{R}_y^{-1}\mathbf{a}(\theta_0)}{\mathbf{a}^H(\theta_0)\mathbf{R}_y^{-1}\mathbf{a}(\theta_0)}. \tag{7}$$

For high signal-to-noise ratio (SNR), relatively low signal-to-interference ratio (SIR), and $N-1 < M$, the output SINR will be very high. The array response pattern magnitude, which is defined by $|G(\theta)| = |\mathbf{w}^H\mathbf{a}(\theta)|$, is such that the SNOI components will probably be almost perfectly nulled[1] $|G(\theta_m)| \approx 0, m \in \{1, \ldots, N-1\}$.

In general, for a beamformer designed to function in a given scenario, subsequent movement of the SOI will result in a pointing error. This can lead to mainlobe signal attenuation effects that decrease output SINR. Moreover, SNOI movement can also very seriously degrade output SINR, especially in those low-noise scenarios where deep nulls are placed at the initial SNOI locations. The problem addressed in this correspondence is *how to broaden the mainlobe and the nulls without knowledge of the SNOI DOA's.* The resulting beamformer, while offering suboptimum SINR performance, possesses greater robustness in the presence of source motion.

[1]Note, however, that this is less likely to be true for moderate or low SNR when one or more SNOI's are close in angle (relative to the array resolution) to the SOI. This is because a null so close to the SOI can produce high sidelobe levels elsewhere in the response that amplify the additive noise term.

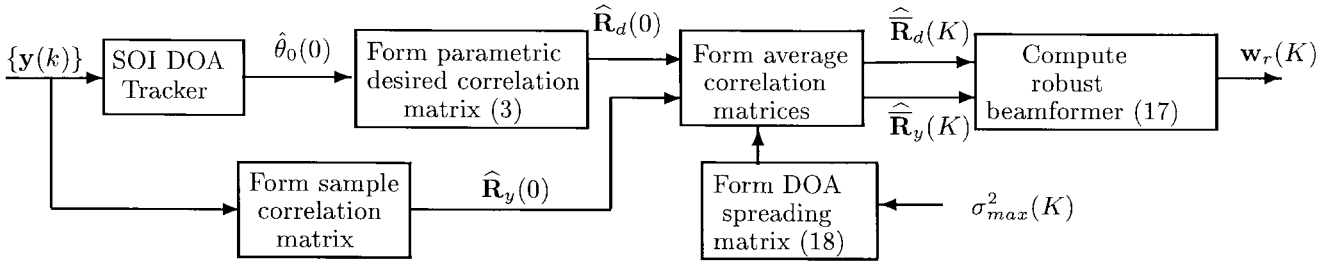

Fig. 1. Block diagram of design procedure.

III. Source Motion and Its Effect on SINR

The loss in performance due to source motion is now quantified. In practice, since such motion is assumed unknown and is not estimated, a model is proposed that simply expresses our lack of precise source DOA knowledge as a function of time. For this purpose, source motion is taken into account by modeling the source DOA's at time $k > 0$ as normal random variables centered on the $k = 0$ DOA's and of time-varying variance

$$\theta_m(k), \sim \mathcal{N}(\theta_m(0), \sigma_m^2(k)), \quad \sigma_m^2(0) = 0 \tag{8}$$

where $\sigma_m^2(k)$, which is the variance of the mth source DOA at time k, is modeled as a monotonically increasing function of k. Again, it is stressed that such a model is not appropriate for describing particular, realistic DOA trajectories. It is, however, a suitable and useful means of expressing our uncertainty as to source DOA, which is induced by source motion for $k > 0$.

A covariance matrix averaged over angle can now be defined as

$$\bar{\mathbf{R}}_y(k) = E_{\theta,k}[\mathbf{R}_y] = \bar{\mathbf{R}}_d(k) + \bar{\mathbf{R}}_{i+n}(k) \tag{9}$$

$$\bar{\mathbf{R}}_d(k) = \gamma_0 \int p\big(\vartheta_0 \mid \theta_0(0), \sigma_0^2(k)\big)\mathbf{a}(\vartheta_0)\mathbf{a}^H(\vartheta_0)d\vartheta_0 \tag{10}$$

$$\bar{\mathbf{R}}_{i+n}(k) = \sum_{m=1}^{N-1} \gamma_m \int p\big(\vartheta_m \mid \theta_m(0), \sigma_m^2(k)\big)\mathbf{a}(v_m) \times \mathbf{a}^H(\vartheta_m)d\vartheta_m + \sigma^2\mathbf{I} \tag{11}$$

where $p(\cdot|\cdot,\cdot)$ is the probability density function of a real Gaussian random variable of specified mean and variance parameters. The above expressions are identical in form to those describing a spatial channel model used to characterize local scattering in mobile communications applications [3]. For the M-element linear uniform array (ULA) with interelement spacing d (relative to the wavelength λ), (9) may be written as [3]

$$\bar{\mathbf{R}}_y(k) = \sum_{m=0}^{N-1} \gamma_m \big[\mathbf{a}(\theta_m(0))\mathbf{a}^H(\theta_m(0))\big] \odot \mathbf{Q}\big(\theta_m(0), \sigma_m^2(k)\big) + \sigma^2\mathbf{I} \tag{12}$$

$$\mathbf{a}(\theta_m(0)) = \big[1, e^{j2\pi d \sin\theta_m(0)}, \ldots, e^{j2\pi d(M-1)\sin\theta_m(0)}\big]^T$$

$$\big[\mathbf{Q}\big(\theta_m(0), \sigma_m^2(k)\big)\big]_{pq} = e^{-2[\pi d(p-q)]^2\sigma_m^2(k)\cos^2\theta_m(0)} \tag{13}$$

where $\odot$, $(\cdot)^T$, and $[\cdot]_{pq}$, respectively, denote the Schur–Hadamard element-by-element matrix product, the vector transpose operation, and the pqth element of a matrix.

A corresponding "average" SINR for this scenario at time k at the output of a beamformer designed at time k' (i.e., which uses data up to time k') can be defined as

$$\overline{\text{SINR}}[k, \mathbf{w}(k')] \equiv \frac{\mathbf{w}^H(k')\bar{\mathbf{R}}_d(k)\mathbf{w}(k')}{\mathbf{w}^H(k')\bar{\mathbf{R}}_{i+n}(k)\mathbf{w}(k')}, \quad 0 \le k' \le k \tag{14}$$

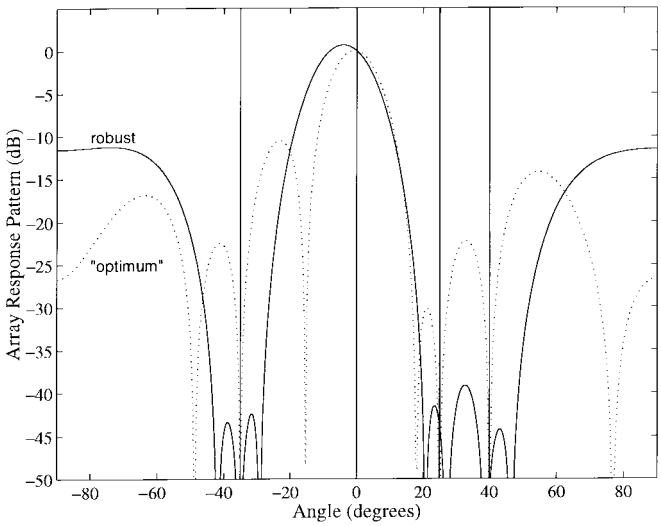

Fig. 2. Array response patterns for conventional optimum beamformer (dotted line) and robust beamformer (solid line). Vertical lines indicate source DOA's.

which is simply the ratio of average signal power to average interference and noise power. Note that, $\overline{\text{SINR}}[k, \mathbf{w_o}(k')]$ is expected to decrease as $k - k'$ increases (i.e., as more time elapses between when the beamformer is designed and when it is used). The next section proposes a new robust beamformer $\mathbf{w}_r(\cdot)$, which, if designed at time $k' = 0$ with the intention of being used over the interval $k \in \{0, \ldots, K\}$, offers the following compromise with respect to the optimum beamformer:

$$\overline{\text{SINR}}[K, \mathbf{w}_o] \le \overline{\text{SINR}}[k, \mathbf{w}_r] < \overline{\text{SINR}}[0, \mathbf{w}_o] = \text{SINR}[\mathbf{w}_o] \tag{15}$$

where all beamformers are designed at $k' = 0$. That is, as the sources move with time, the robust beamformer will perform better than the optimum beamformer but at the cost of suboptimum initial performance.

IV. Robust Beamformer

The robust beamformer presented in this section will be based on the source motion model as reflected in the average covariance matrix of (12). The effect of the associated "DOA spreading matrix" as defined in (13) is to smear or spread the point sources over intervals centered on the initial ($k = 0$) DOA's. A beamformer that is designed to be robust in the presence of source motion should take this smearing effect into account in order to create a broad mainlobe for the desired user and broad nulls for the interfering users. To this end, we can define the optimum robust constrained minimum variance (i.e., maximum $\overline{\text{SINR}}$) beamformer as the solution of the following

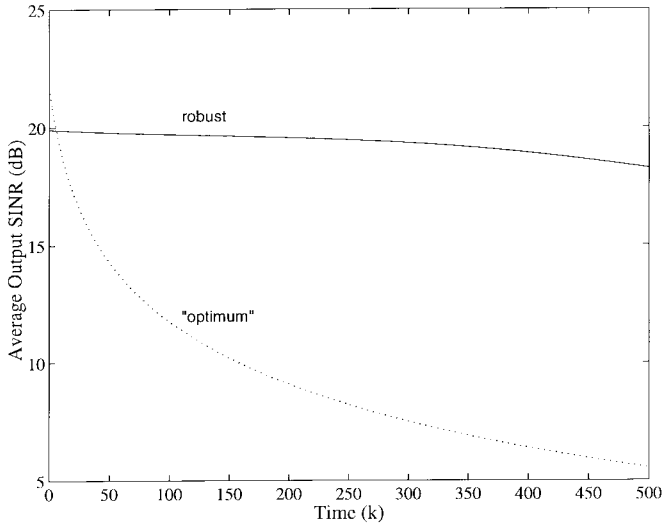

Fig. 3. Average output SINR versus time for conventional optimum beamformer (dotted line) and robust beamformer (solid line).

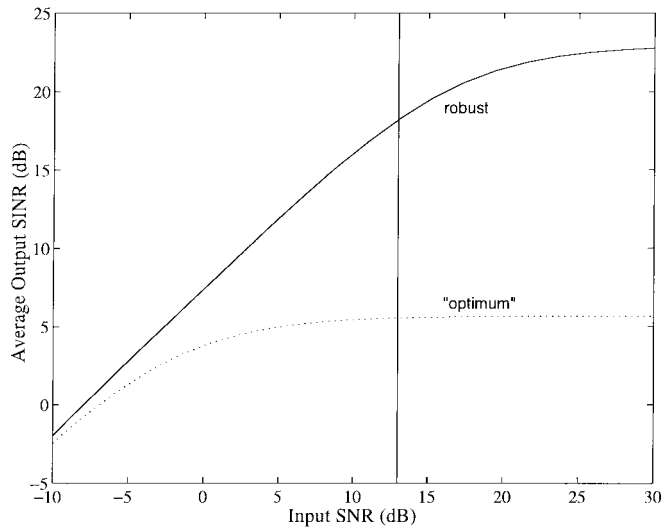

Fig. 4. Average Output SINR at $k = K = 500$ versus input SNR for conventional optimum beamformer (dotted line) and robust beamformer (solid line). The vertical line corresponds to the input SNR for the scenario considered in Figs. 1 and 2.

constrained minimization problem:

$$\mathbf{w}_r(k) = \arg\min_{\mathbf{w}} \mathbf{w}^H \bar{\mathbf{R}}_y(k)\mathbf{w} \quad \text{subject to} \quad \mathbf{w}^H \bar{\mathbf{R}}_d(k)\mathbf{w} = \gamma_0. \tag{16}$$

In contrast to (6), the quadratic constraint in (16) cannot be expressed as a linear constraint because, in general, $\text{rank}(\bar{\mathbf{R}}_d(k)) > 1$ for $k > 0$. In such a case, (16) is solved via a straightforward application of generalized eigenanalysis

$$\mathbf{w}_r(k) = \mathbf{e}_{\max} \sqrt{\frac{\gamma_0}{\mathbf{e}_{\max}^H \bar{\mathbf{R}}_d(k) \mathbf{e}_{\max}}} \tag{17}$$

where $\mathbf{e}_{\max}$ is the generalized eigenvector associated with the maximum generalized eigenvalue of the matrix pair $\{\bar{\mathbf{R}}_d(k), \bar{\mathbf{R}}_y(k)\}$. This beamformer should have the effect of broadening the mainlobe as well as the potentially sharp nulls that would have been placed over the SNOI's by the ordinary optimum beamformer.

The spreading matrix (13) is a function of source DOA at $k = 0$ and the angular perturbation variance for each source. To avoid

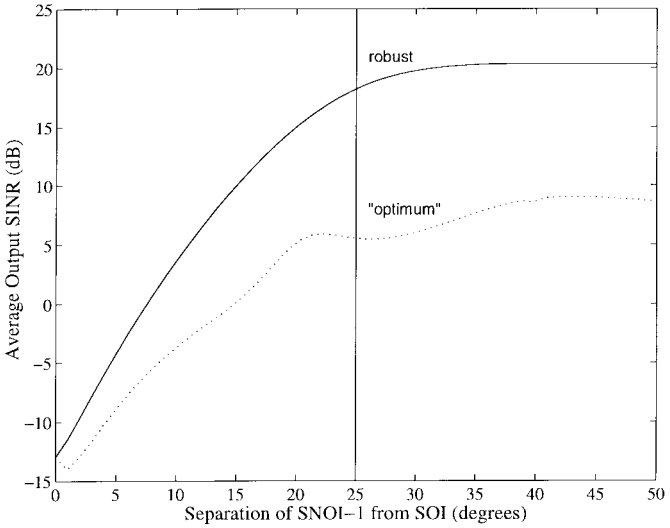

Fig. 5. Average Output SINR at $k = K = 500$ versus SOI-SNOI-1 angular separation for conventional optimum beamformer (dotted line) and robust beamformer (solid line).The vertical line corresponds to the angular separation for the scenario considered in Figs. 1 and 2.

estimation of the DOA's of the SNOI's and the angular perturbation variances of all the sources, consider a pessimistic, worst-case spreading matrix

$$[\tilde{Q}(K)]_{pq} = e^{-2[\pi d(p-q)]^2 \sigma^2_{\max}(K)} \tag{18}$$

where $\sigma^2_{\max}(K)$ is an upper bound on the angular perturbation variance.[2] Then, from (9) and (12), the average covariance matrices required to design the beamformer can be computed as follows:

$$\bar{\mathbf{R}}_d(K) = \mathbf{R}_d(0) \odot \tilde{Q}(K), \qquad \bar{\mathbf{R}}_y(K) = \mathbf{R}_y(0) \odot \tilde{Q}(K). \tag{19}$$

The overall design procedure is described in Fig. 1. The snapshot data $\mathbf{y}(k)$ is collected over $k \in \{-L+1, \ldots, 0\}$, which is some interval during which all the source angles do not change significantly. This data is applied to a DOA estimation/tracking algorithm (e.g., [6]) to yield an estimate of the initial SOI DOA, $\hat{\theta}_0(0)$, which, in turn, is used to form $\hat{\mathbf{R}}_d(0) = \mathbf{a}(\hat{\theta}_0(0))\mathbf{a}^H(\hat{\theta}_0(0))$, which is a parametric estimate of the SOI correlation matrix.[3] The snapshot data is also used to form the full sample correlation matrix as $\hat{\mathbf{R}}_y(0) = \frac{1}{L}\sum_{k=-L+1}^{0} \mathbf{y}(k)\mathbf{y}^H(k)$. Next, after choosing a worst-case angular spreading variance $\sigma^2_{\max}(K)$, the corresponding DOA spreading matrix $\tilde{\mathbf{Q}}(K)$ is computed via (18). This matrix, along with $\hat{\mathbf{R}}_d(0)$ and $\hat{\mathbf{R}}_y(0)$, are then used to calculate estimates of the average desired and full correlation matrices $\hat{\bar{\mathbf{R}}}_d(K)$ and $\hat{\bar{\mathbf{R}}}_y(K)$ via (19). Last, the robust beamforming weight vector $\mathbf{w}_r(K)$ is computed via (17) as a scaled version of the generalized eigenvector associated with the maximum eigenvalue of the matrix pair $\{\hat{\bar{\mathbf{R}}}_d(K), \hat{\bar{\mathbf{R}}}_y(K)\}$.

An important feature of the proposed criterion (16) is that the resulting beamformer makes "intelligent" use of its degrees of freedom to minimize noise and interference. The effects of additive noise, source motion, and potentially large differences in source powers (i.e., the so-called "near-far effect") are all taken into account. For example, relatively more degrees of freedom will be automatically

[2]This approximation will have the effect of somewhat overestimating the angular perturbation for sources near endfire and/or sources moving "slowly" relative to the speed implied by $\sigma^2_{\max}(K)$. However, in networks employing *cell sectorization* (e.g., 120° per sector in GSM [5]), the former source of inaccuracy will be less pronounced.

[3]In fact, a *unit power* version of this matrix is formed. The constraint in (16) is such that explicit knowledge SOI power is not required.

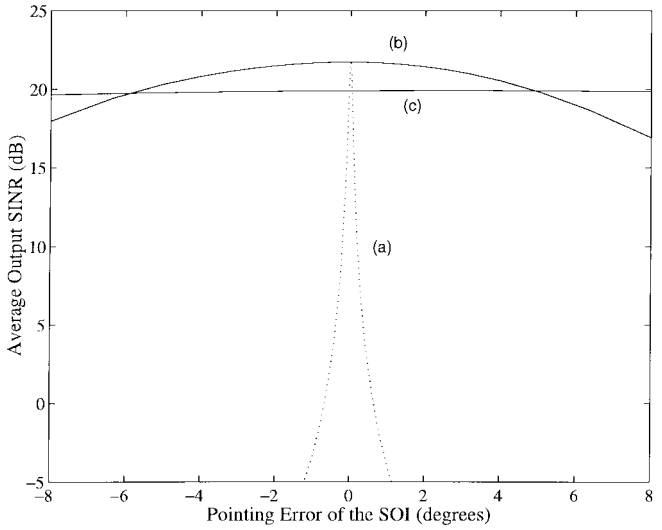

Fig. 6. Average output SINR for robust beamformer at $k = 0$ versus SOI pointing error. (a) $\sigma_{\max} = 0$ (optimum beamformer). (b) $\sigma_{\max} = 0.07^\circ$. (c) $\sigma_{\max} = 7^\circ$.

allocated for the suppression of a particular interferer as its power increases.

V. Results

Computer simulations results now illustrate the performance of the new technique. Consider $N = 4$ sources (one SOI and three SNOI's) impinging on a uniform linear array of $M = 8$ sensors with half-wavelength interelement spacing. The initial DOA's of the SOI and the three SNOI's at time $k = 0$ are, respectively, $\theta_0(0) = 0^\circ$, $\theta_1(0) = 25^\circ$, $\theta_2(0) = 40^\circ$, and $\theta_3(0) = -35^\circ$. The source powers are $\gamma_0 = 1$, $\gamma_1 = \gamma_2 = \gamma_3 = 20$. The sensor noise power is $\sigma^2 = 0.05$. The resulting SNR's are 13 dB for the SOI and 26 dB for each of the three SNOI's. The corresponding SINR is -17 dB. The performance of the proposed beamformer is considered over a period of $K = 500$ output samples during which the sources undergo random DOA perturbations in angle with time K standard deviations: $\sigma_0(K) = 5.1^\circ$, $\sigma_1(K) = 5.6^\circ$, $\sigma_2(K) = 6.7^\circ$, and $\sigma_3(K) = 6.3^\circ$. The new technique is applied to this scenario assuming $\sigma_{\max}(K)$ of (18) is set to 7°.[4]

Fig. 2 shows the broad mainlobe and broad nulls placed by the robust beamformer at the angles of the desired user and the interferences, respectively. This is to be compared with the narrower mainlobe and sharper nulls created by the conventional optimum beamformer. Fig. 3 compares the average output SINR as a function of time from which the beamformer is designed for the optimum and the robust beamformer. In this example, we have assumed that the angular variances increase linearly with time (i.e., $\sigma_m^2(k) = \sigma_m^2(K)k/K,\ k \in \{0, 1, \ldots, K\}$). It is seen that although the optimum beamformer designed at time $k = 0$ yields very high initial performance, this steadily degrades with time as the SNOI's move further away from the nulls present in the array response pattern. On the other hand, the robust beamformer performance remains roughly constant with time; it is initially somewhat inferior to that of the optimum beamformer designed at $k = 0$ but quickly offers greatly improved performance as a function of time due to the wider nulls present in its array response pattern. Fig. 4 shows the effect of the sensor noise power on output SINR at time $k = K$. As expected, the robust beamformer performance gain diminishes as input SNR decreases. Fig. 5 shows the time $k = K$ performance as the initial $(k = 0)$ DOA as the first SNOI approaches that of the SOI. As a broad null is created at the SNOI angle, the SOI is also attenuated if the SNOI and SOI angles are close. This implies that the robust beamformer performance gain worsens as the angular separation decreases. Last, Fig. 6 shows the sensitivity of the robust beamformer to initial SOI DOA pointing errors. Performance is calculated at time $k = 0$ (when the only source of error would be that due to pointing errors). It is seen that the robust beamformer, even with low assumed spreading, is far less sensitive to initial pointing errors.

[4]It is noted that a movement of 7° during $K = 500$ snapshots starting from broadside and assuming a sampling rate of 10 kHz implies that a source 2.5 km from the array would move with a mean speed of approximately 22 km/hr.

VI. Conclusion

A new method for the design of beamformers that are robust in the presence of source motion was presented. The technique is useful in mobile communications applications where the beamforming weights are frozen for some length of time (despite changes in the scenario) before being updated. The new beamformer is easily implemented and was seen to offer a dramatic improvement in performance with respect to the optimum beamformer in the presence of source movement for several scenarios.

References

[1] J. H. Winters, "Signal acquisition and tracking with adaptive arrays in the digial mobile radio system IS-54 with flat fading," *IEEE Trans. Veh. Technol.*, vol. 42, pp. 377–384, Nov. 1993.

[2] W. C. Jakes, *Microwave Mobile Communications*. New York: Wiley, 1974.

[3] P. Zetterberg and B. Ottersten, "The spectrum efficiency of a basestation antenna array system for spatially selective transmission," *IEEE Trans. Veh. Technol.*, vol. 44, pp. 651–660, Aug. 1995.

[4] A. B. Gershman, G. V. Serebryakov, and Johann F. Böhme, "Constrained Hung–Turner adaptive beam-forming algorithm with additional robustness to wideband and moving jammers," *IEEE Trans. Antennas Propagat.*, vol. 44, no. 3, pp. 361–367, Mar. 1996.

[5] S. M. Redl, M. K. Weber, and M. W. Oliphant, *An Introduction to GSM*. Norwood, MA: Artech House, 1995, p. 31.

[6] J. Riba, J. Goldberg, and G. Vàzquez, "Signal selective DOA tracking for multiple moving targets," in *Proc. IEEE ICASSP*, vol. V, May 1996, pp. 2559–2562.